Digest Journal of Nanomaterials and Biostructures Vol. 12, No. 2, April - June 2017, p. 463 - 471

FIRST-PRINCIPLE STUDY OF THE INTERACTION BETWEEN GRAPHENE AND METALS

X. M. DU*, K. F. ZHENG, R. Q. CHEN, F. G. LIU
School of Materials Science and Engineering, Shenyang Ligong University, Shenyang 110159, China

First principles density functional theory with ultrasoft pseudopotentials constructed with the local density approximation is used to investigate interfacial bonding at Al(111)/graphene, Cu(111)/graphene and Mg(0001)/graphene interfaces. The calculated results of the interface binding energies and interface distances indicate that the interfacial bonding between graphene and Al, Mg is weaker than the metallic bonding within the Al or Mg slabs, whereas the interfacial bonding between graphene and Cu is of the same magnitude as that between the basal planes in Cu slab. The band structure, the density of state and contours of the electron density also reveal that the chemical bondings are formed between the graphene and Cu slab, whereas the interactions between graphene and Al (or Mg) slabs are in Van Der Waals force range. Our works provide a detailed understanding of the interfacial properties of metal-graphene composit materials, and help to obtain an insight into strengthening mechanism of graphene on metal matrix. The availability of structural, energetic and electronal structure data of metal-graphene interfaces could also be useful for the development of novel graphene reinforced composite materials.

(Received February 19, 2017; Accepted May 24, 2017)

Keywords: Metal/graphene composite; interfacial bonding; first-principle calculation

1. Introduction

Successful isolation of the graphite monolayer, graphene, in 2004 has opened up a new field of research [1,2], and has attracted much attention as a fascinating candidate for nanoelectronics and spintronics [3-6] due to its excellent properties. In addition, higher strength and toughness are also the potential advantage of graphene in engineering application [7,8]. Much research effort has been devoted to the study of interaction between graphene and metal surfaces [9-12], and other dielectric surfaces. These graphene–substrate interactions are of practical significance during the process of graphene synthesis and graphene-based composite materials fabrication. In particular, metal-graphene interfaces are formed and used in material production [10,13], electrical measurement[11].

In experimental studies [14-17], it is shown that the graphene at the metal–graphene interfaces can significantly improve mechanical properties, such as strength, toughness, hardness, and tribological property of the metal-based composite materials. Recent experimental studies of metal–graphene interfaces have also shown that different metals show different interfacial bonding (strong for Ni and Ti/Au and weak for Pt and Au) and that carbide bonds are formed at Ti–G but not at Pt–G interfaces [18]. Density functional theoretical (DFT) studies have proven to be quite useful for understanding the thermodynamic and electronic behaviors at bi-material interfaces. DFT study of metal-graphene interfaces has shown that the metal substrate and graphene can form either a

* Corresponding author: du511@163.com

physisorption interface with charge transfer [19,20] or a chemisorption interface with orbital hybridization [21-23]. While chemisorption opens a band gap in graphene due to hybridization between the graphene p_z-orbital and metal *d*-orbital, the Dirac-cone feature of graphene is preserved at the physisorbed interfaces. Subsequent investigations illustrated that physisorption is observed for Ag, Al, Cu, Cd, Ir, Pt, and Au, whereas the Ni, Co, Ru, Pd, and Ti interfaces belong to chemisorption [24-26]. These studies play an important role in understanding the electron transport behavior of graphene/metal composites. However, the investigation of the influence of graphene/metal interfaces on the stability and mechanical properties of the composites is very little. Particularly, the detailed atomic scale investigations based on DFT studies are currently lacking, and the physical and electronic behaviors of these interfaces are not yet well understood.

In the present work, we use first-principle methods to gain a fundamental understanding of the energetic and electronic properties of metal/graphene composits. We focused primarily on computing interfacial bonding at Al(111)/graphene, Cu(111)/graphene and Mg(0001)/graphene interfaces, by considering Al, Cu, Mg and their interactions with graphene in order to provide a fundamental perspective of their structure and properties.

2. Computational details

The lattice parameters of fcc-Al, fcc-Cu, hcp-Mg were molded according to the literatures [27-29]. The bulk calculations were conducted on graphene, aluminum, copper and magnesium primitive cells to assess the accuracy of our computational methodology.

The clean Al(111), Cu(111) and Mg(0001) surfaces were modeled using a (2×2), (1×1) and (3×3) surface unit cells, respectively, with six atomic layers and a vacuum distance of 15Å. The heterogeneous system of interest is graphene on the (111) surface of aluminum, copper and (0001) surface of magnesium.

If the lattice constant of graphene is fixed at the optimized value 2.45 Å, less than 5% lattice mismatch is introduced when these metals of face-centered cubic symmetry are made commensurate with the graphene lattice. The supercells used to model the metals/graphene interfaces are constructed from a slab of six layers of metal atoms with a graphene sheet and a 15 Å vacuum layer, which is large enough to guarantee a sufficient separation between periodic images. The graphene honeycomb lattice then matches the triangular lattice of the metals (111) and (0001) surfaces in the lateral unit cells shown in Fig. 1. The diamond frame in the Fig.1 represents the primary unit cell of the various interfaces. For the Al(111)/graphene interface, a $2\times2\angle30°$ graphene supercell is used to match to Al(111) slab. The C atoms occupy on the top (*A* site) and bridge (*B* site) sites of the Al(111) slab. For the Cu(111)/graphene interface, a graphene primitive cell is used to match to Cu(111) slab. The C atoms occupy on the top (*A* site) and hollow (*C* site) sites of the Cu(111) slab. For the Mg(0001)/graphene interface, a 4×4 graphene supercell is used to match to Al(111) slab. The C atoms occupy many sites on Mg(0001) slab, including the top and bridge sites.

We calculate DFT ground-state energies, and optimized geometries using a plane-wave basis set at the level of the local density approximation (LDA) [30] as implemented in Quantum-ESPRESSO program package [31]. The plane-wave kinetic-energy cutoff is set at 400 eV. To check the validity of our approach, we computed selected bulk properties of aluminum, copper, magnesium

and graphene using a ultrasoft pseudopotential. The same pseudopotential was used to compute the energetics and geometries of Al(111)/graphene, Cu(111)/graphene and Mg(0001)/graphene. All calculations were conducted with the LDA adapted by Ceperley and Alder [32]. The Brillouin Zone integrations were performed using the Monkhorst-Pack [33] k-point meshes, e.g., the k-point meshes for fcc-crystals and hcp-cryatals bulk calculations were set to 8×8×8 and 8×8×6, respectively. A (5×5×1) Monkhost-Pack grids was used in the Brilluion-zone sampling for each surface. The k-point meshes for Al(111)/graphene, Cu(111)/graphene and Mg(0001)/graphene interfaces calculations were set to 5×5×1, 5×5×1and 3×3×1, respectively.

All lattice parameters and atomic positions in our models have been relaxed according to the total energy and force using the Broyden-Flecher-Goldfarb-Shanno (BFGS) [34] scheme. The convergence criteria for geometry optimization was as follows: electronic self-consistent field (SCF) tolerance less than 5.0×10^{-5} eV/atom, Hellmann-Feynman force below 0.01eV/Å, maximum stress less than 0.05GPa and displacement within 2.0×10^{-4} Å. After the structures were optimized, the total energies were recalculated self-consistently with the tetrahedron method. The latter technique was also used to calculate the electronic structure properties.

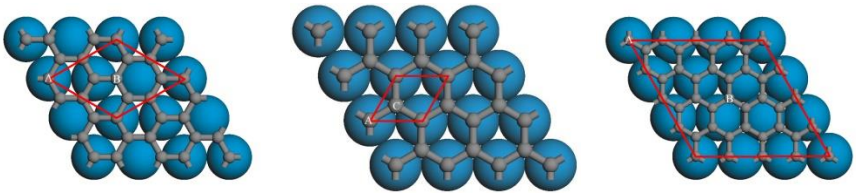

(a) *(b)* *(c)*

Fig. 1. Interface models of metals/graphene interfaces, (a) Al (111)/graphene (b) Cu (111)/graphene and (c) Mg(0001)/graphene, the most stable symmetric configuration of graphene on Al(111), Cu (111) and Mg(0001) has one carbon atom on top of a metal atom (A site), and the second carbon on a bridge or hollow site (B or C site).

3. Results and discussions

3.1 Bulk calculations

The calculated equilibrium lattice constants, the equilibrium cell energies, and the cohesive energies for fcc-Al, fcc-Cu, hcp-Mg and graphene studied in this paper are listed in Table 1, where the available experimental results are also presented. It can be found that the present calculated lattice constants and cohesive energies are in good agreement with the available experimental values [27-29], with a difference within 3.0%, confirming that the computational methodology utilized in this work is highly suitable and reliable.

Table 1. Results for fcc-Al, fcc-Cu, hcp-Mg and graphene including equilibrium lattice constants, total energy E_{tot} and cohesive energy E_{coh}

Materials	Space group	Lattice parameter (Å)				Volume (Å^3)	Total energy E_{tot} (eV/f. u.)	E_{coh} (eV·atom^{-1})
		Present		Experimental				
		a	*c*	*a*	*c*			
Fcc-Al	Fm-3m	4.116		4.049 [a]		69.747	-223.8348	-3.22 (-3.39[d])
Fcc-Cu	Fm-3m	3.529		3.615 [b]		43.958	-5907.5612	-6.02
Hcp-Mg	P63/mmc	3.165	5.363	3.213 [c]	5.213[c]	42.526	-1946.1259	-1.477 (-1.51[e])
Graphene		2.45					-311.0473	-10.35

[a] Ref.[27], [b] Ref.[28], [c] Ref.[29], [d] Ref.[35], [e] Ref. [36].

3.2 Surface calculations

Surface relaxation calculations for all materials were performed to determine surface thickness. The *n*-layer (*n*=3,4,5,6,7) Al(111) and Cu(111) slabs with one atom per layer and Mg (0001) slab with two atoms per layer were created, respectively. The surface thickness was determined via convergence of the surface energy using the method of Boettger [37], which is summarized by Eq. (1):

$$H_s = \frac{1}{2}[H_n - \frac{n}{2}(H_N - H_{N-2})] \quad (1)$$

where H_s is the surface energy, H_n is the energy of a lab having a thickness of *n*-atomic layers, and $H_N - H_{N-2}$ is the average of all $H_n - H_{n-2}$ values for each value of *n*, where $n > 2$. The surface energy intensity was obtained by dividing H_s by the area of the surface. Convergence was defined at the 0.01 J/m^2 level. The calculated results of surface energies for surface thickness convergence are listed in Table 2. As shown in Table 2, the surface energy converged to 1.46 J/m^2, 6.83 J/m^2 and 4.04 J/m^2, for an 6-layer Al(111) and Cu(111) and Mg (0001) slabs, respectively, and these were subsequently used for the metals/graphene interfaces (as shown in Fig.1) calculations.

Table 2 Surface energies (J/m^2) as a function of thickness for Al(111), Cu(111) and Mg(0001)

Surface thickness (atomic layer *n*)	Al(111) surface energy	Cu(111) surface energy	Mg(0001) surface energy
3	-1.65	-7.13	-2.10
4	-1.54	-8.45	-3.36
5	-1.49	-6.98	-3.12
6	-1.46	-6.83	-4.04
7	-1.46	-6.83	-4.04

3.3 Composite Interfaces

We initially placed the flat graphene sheet close to the top metal layer at a height of 2.5 Å

to optimize a suitable interfacial distance between graphene and metal. This initial distance is much shorter than one half of the sum of graphite and metal substrate's interlayer spacings (2.85 Å, 2.71 Å and 3.04 Å for Al (111), Cu(111) and Mg(0001), respectively). The calculated equilibrium interface distances between graphene and metals studied in this paper are listed in Table 3. For weak interaction interfaces between graphene and metals (Al and Mg), binding energies of Al(111)/graphene and Mg(0001)/graphene are -0.243 and -0.079 eV per carbon atom, respectively. For the case with a smaller interface binding energy and a larger interface distance, there possiblely exists Van Der Waals interactions between graphene and metals interfaces. The minimized interfacial distances of 3.66 Å and 3.50 Å for Al(111)/graphene and Mg (0001)/graphene were larger than the 2.38 Å and 2.74 Å final distances between the Al(111) planes and Mg (0001) planes, respectively. This lends some credence to the possibility that the interfacial bonding between the two materials is weaker than the metallic bonding within the Al or Mg slabs. These basic findings are consistent with experimental observations and theoretical calculations in the recent works [38,39,40]. For strong interaction interfaces between graphene and copper, the binding energy is -0.808 eV per carbon atom. After minimization, the interfacial distance (2.06 Å) was similar to the distance between the Cu(111) planes (i.e. 2.087 Å), suggesting the interfacial bonding is of the same magnitude as that between the basal planes in Cu slab. Many researchers think that the smaller equilibrium interface distances and the larger binding energy between metals and graphene interfaces can form a chemical bonding (or chemisorption) [41-45].

Table 3 The structural and energetic parameters of the optimized interfaces

Interfaces	The interface distances (Å)	Binding energy (eV/C atom)
Al(1 1 1)/graphene	3.66	-0.243
	3.59[38]	
	3.41[39]	
Cu(1 1 1)/graphene	2.06	-0.808
	2.96[38]	
	3.26[39]	
	2.24[40]	
Mg(0 0 0 1)/graphene	3.50	-0.079

The calculated electronic band structures of graphene and metal/graphene interfaces are shown in Fig. 2. The band structure for graphene shown in Fig. 2(a) is actually calculated for a periodic structure where graphene monolayers are separated by the same vacuum distance as for the graphene/metal slabs. This band structure shows the crossing of the π and π* bands at the *K* point and at the Fermi energy (the characteristic conical points of graphene at *K* are formed) as well as the flat unoccupied σ* band at about 8.0 eV above E_F.

For Cu(111)/graphene with the larger binding energy, the graphene bands are strongly perturbed. In particular, the characteristic conical points of graphene at *K* are destroyed, as shown in Fig 2(c). Graphene *p* orbits hybridize strongly with the Cu *d* orbits and the corresponding bands acquire a mixed graphene-metal character. It demonstrates that the chemical bondings are formed

between the graphene and the Cu(111) slab. In contrast, if the metal-graphene interaction is weaker, i.e., Al(111)/graphene and Mg(0001)/graphene, the graphene bands, including their conical points at *K*, can still be clearly identified, as shown in Fig. 2(c) and (d). It is indicated that there is no chemical bonding between graphene and metals. Unlike the case of graphene where the Fermi level coincides with the conical point, metal-graphene interfaces generally deviate from the Fermi level (Fig. 2(c) and (d)).

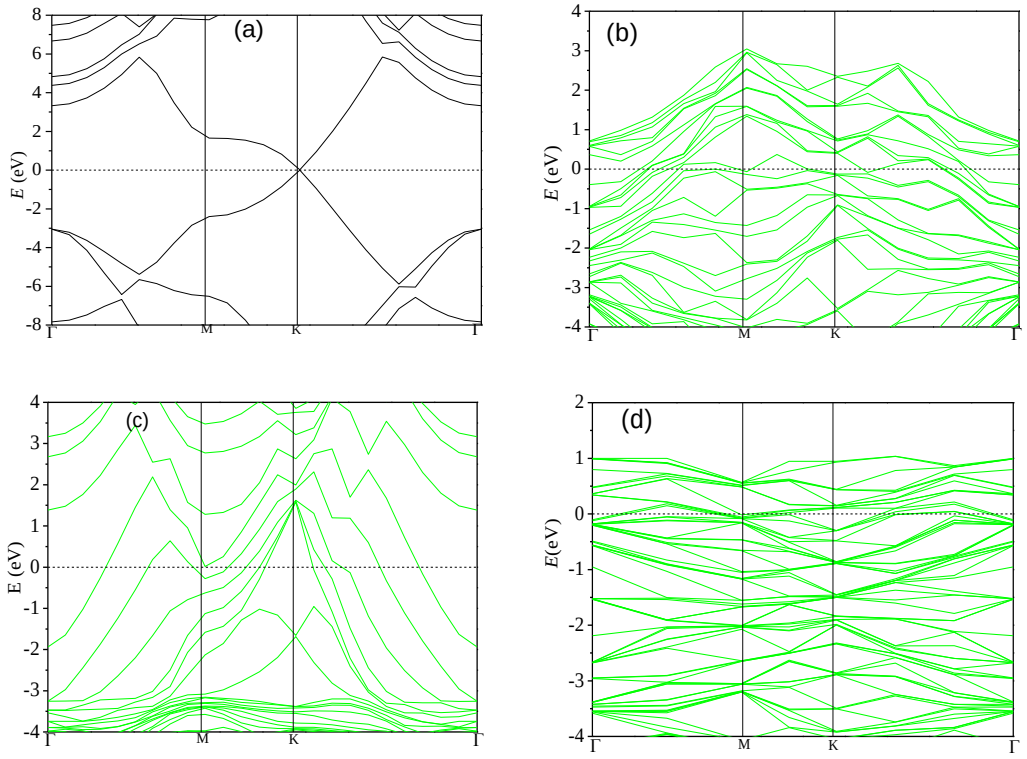

Fig. 2 Band structures of metal/graphene interfaces, (a) graphene, (b) Al (111)/graphene (c) Cu (111)/graphene and (d) Mg(0001)/graphene. The Fermi level is at zero energy.

In the present work, the density of state was also calculated to gain a further insight into the bonding of metal/graphene interfaces, and then to reveal the underlying structural stability mechanism of these interfaces. The total and partial densities of states (DOS and PDOS) of these interfaces are presented in Fig. 3. From Fig.3 (a), it is found that the main peaks of DOS on Al(111)/graphene interface locate in the range from −11 eV to 0 eV, originating from the contribution of valance electron numbers of Al-3p, Al-3s and C-2p orbits. No typical hybridization peaks were observed. For the range below -11 eV, total DOS origins from the contribution of valance electron numbers of C-2s and C-2p orbits. There exists a valley on Fermi level for total DOS plot, also called pseudogap, which of the width directly determines the strength of the interaction of covalent bonds in the system or between the two atoms. However, the pseudogap is very narrow for Al(111)/graphene interface. It is indicated that the interaction between neighboring Al atoms and C atoms is weak. For Cu(111)/graphene interface, it is found that total DOS (from -11eV to 0 eV) origins from the contribution of valance electron of Cu-3d and C-2p orbits, as shown in Fig. 3(b). The 3d orbit electrons of Cu atoms increase the number of state on valence band. The PDOS of the C atom expands, and the number of states in the conduction band increases. An obvious

hybridization peak caused by the valance electron of Cu-3d and C-2p orbits appears near the Fermi level. It is indicated that the chemical bonds appear between Cu atoms and C atoms. The characteristics of DOS in Mg (0001)/graphene interface is similar with that of Al(111)/graphene interface (Fig. 3(c)).

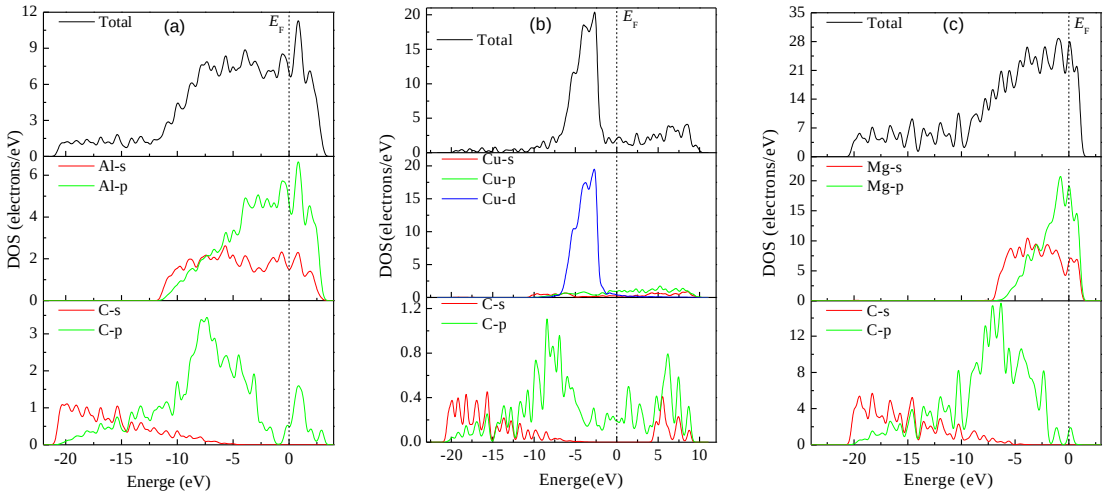

Fig.3 The DOS of metal/graphene interfaces, (a) Al (111)/graphene (b) Cu (111)/grapheme and (c) Mg(0001)/graphene

To visualize the nature of the bonding character and to explain the charge transfer and the bonding properties of the metal/graphene interfaces, we have also investigated change of the charge density distribution of three metal/graphene interfaces. Fig. 4 shows the charge-density contours on the (110) plane. It is found from Fig. 4 (a) and (c) that there is almost no overlap of electronic cloud between the C atoms in graphene and the neighboring Al (or Mg) atoms, showing the interactions between C and Al (or Mg) atoms are in Van Der Waals range. However, the electron cloud between C atoms and Cu atoms on the interface overlaps, as shown in Fig. 4 (b). It shows that there is strong interaction between graphene and Cu(111) slab. These results obtained from the electron structure properties are consistent with that of the binding energies.

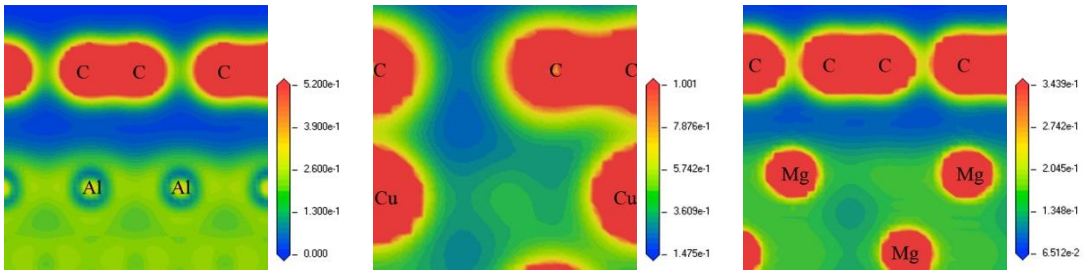

(a) Al (111)/graphene *(b) Cu (111)/graphene* *(c) Mg(0001)/graphene*

Fig.4 The electron density of metal/graphene interface on (110) plane

4. Conculsions

Using plane wave density functional theory with ultrasoft pseudopotentials based upon the local density approximation, we studied the interfacial bonding at Al(111)/graphene, Cu(111)/graphene and Mg(0001)/graphene interfaces. The calculated results of the interfacial binding energies and interface distances lend some credence to the possibility that the interfacial bonding between graphene and Al, Mg is weaker than the metallic bonding within the Al or Mg slabs, whereas the interfacial bonding between graphene and Cu is of the same magnitude as that between the basal planes in Cu slab. The band structure, the density of state and contours of the electron density also reveal that the chemical bondings are formed between the graphene and Cu slab, whereas the interactions between graphene and Al (or Mg) slabs are in Van Der Waals force range.

Acknowledgements

This work is supported by the Natural Science Foundation of Liaoning (201602642), Scientific Fund of Liaoning Provincial Education Department (LG201620).

References

[1] K. S. Novoselov, A. K. Geim, S. V. Morozov, D. Jiang, Y. Zhang, S. V. Dubonos, I. V. Grigorieva, and A. A. Firsov, Science **306**, 666 (2004).
[2] A. K. Geim, K. S. Novoselov, Nat. Mater. **6**, 183 (2007).
[3] M. I. Katsnelson, Mater.Today **10**, 20 (2007).
[4] A. H. CastroNeto, F. Guinea, N. M. R. Peres, K. S. Novoselov, A. K. Geim, Rev. Mod. Phys. **81**, 109 (2009).
[5] M. Ishigami, J. H. Chen, W. G. Cullen, M. S. Fuhrer, E. D. Williams, NanoLett. **7**, 1643 (2007).
[6] J. Wu, W. Pisula, K. Müllen, Chem. Rev. **107**, 718 (2007).
[7] C. G. Lee, X. D. Wei, J. W. Kysar, J. Hone, Science **321**, 385 (2008).
[8] G. H. Lee, J. Hone, Science **340**, 1073 (2013).
[9] G. Bertoni, L. Calmels, A. Altibelli, and V. Serin, Phys. Rev. B **71**, 075402 (2005).
[10] P. W. Sutter, J.-I. Flege, and E. A. Sutter, Nature Mater. **7**, 406 (2008).
[11] B. Huard, N. Stander, J. A. Sulpizio, and D. Goldhaber-Gordon, Phys. Rev. B **78**, 121402 (2008).
[12] S. Barraza-Lopez, M. Vanevic, M. Kindermann, and M. Y. Chou, Phys. Rev. Lett. **104**, 076807 (2010).
[13] X. Li, W. Cai, J. An, S. Kim, J. Nah, D. Yang, R. Piner, A. Velamakanni, I. Jung, E. Tutuc, S. K. Banerjee, L. Colombo, and R. S. Ruoff, Science **324**, 1312 (2009).
[14] J. Wang, Z. Li, G. Fan, H. Pan, Z. Chen, D. Zhang, Scr. Mater. **66**, 594 (2012).
[15] L.Y. Chen, H. Konishi, A. Fehrenbacher, C. Ma, J. Q. Xu, H. S. Choi, H. F. Xu, F. E. Pfefferkorn, X. C. Li, Scr. Mater. **67**, 29 (2012).
[16] A. F. Boostani, S. Yazdani, R. T. Mousavian, S. Tahamtan, R. A. Khosroshahi, D. Wei, D. Brabazon, J. Z. Xu, X. M. Zhang, Z. Y. Jiang, Materials and Design **88**, 983 (2015).
[17] H. Y. Yue, L. H. Yao, X. Gao, S. L. Zhang, E. J. Guo, H. Zhang, X. Y. Lin, B. Wang, J. Alloys Compd. **691**, 755 (2017).

[18] A. Pirkle, R. M. Wallace, and L. Colombo, Appl. Phys. Lett. **95**, 133106 (2009).
[19] I. Pletikosić, M. Kralj, P. Pervan, P. Brako, J. Coraux, A. T. N'Diaye, C. Busse, T. Michely, Phys. Rev. Lett. **102**, 056808 (2009).
[20] S. Barraza-Lopez, M. Vanevic, M. Kindermann, M. Y. Chou, Phys. Rev. Lett. **104**, 076807 (2010).
[21] Q. J. Wang, J. G. Che, Phys. Rev. Lett. **103**, 066802 (2009).
[22] A. Varykhalov, J. Sánchez-Barriga, A. M. Shikin, C. Biswas, E. Vescovo, A. Rybkin, D. Marchenko, and O. Rader, Phys. Rev. Lett. **101**, 157601 (2008).
[23] A. Grüneis, D. V. Vyalikh, Phys. Rev. B **77**, 193401 (2008).
[24] Q. Ran, M. Gao, X. Guan, Y. Wang, Z. Yu, Appl. Phys. Lett. **94**, 103511 (2009).
[25] C. Gong, G. Lee, B. Shan, E. M. Vogel, R. M. Wallace, K. Cho, J. Appl. Phys. **108**, 123711 (2010).
[26] C. Gong, D. Hinojos, W. Wang, N. Nijem, B. Shan, R. M. Wallace, K. Cho, Y. J. Chabal, ACS Nano **6**, 5381 (2012).
[27] S. Popovic, B. Grzeta, V. Ilakovac, R. Kroggel, G. Wendrock, H. Löffler, Phys. Status Solidi A **130**, 273 (1992).
[28] R. P. Van Ingen, R. H. J. Fastenau, E. J. J. Mittemeijer, Appl. Phys. **76**, 1871 (1994).
[29]J. Karen P., A. Kjekshus, Q. Huang, V. L. Karen, J. Alloys Compd. **282**, 72 (1999).
[30] J. P. Perdew, A. Zunger, Phys. Rev. B **23**, 5048 (1981).
[31] http://www.pwscf.org.
[32] D. M. Ceperley, B. J. Alder, Phys. Rev. Lett. **45**, 566 (1980).
[33] H. J. Monkhorst, J. D. Pack, Phys. Rev. B **13**, 5188 (1976).
[34] T. H. Fischer, J. Alml, J. Phys. Chem. **96**, 9768 (1992).
[35] L. Brewer, LBL Report, (1975) 3720.
[36] C. Kittel, Introduction to Solid State Physics, 7th ed. (Wiley, New York, 1996).
[37] J. C. Boettger, Phys. Rev. B **49**, 16798 (1994).
[38] C. Gong, G. Lee, B. Shan, J. Appl. Phys. **108**, 1859 (2010).
[39] P. C. Rusu, Phys. Rev. B Condensed Matter **79**, 195425 (2009).
[40] Z. Xu, M. J. Buehler, J. Phys. Condensed Matter **22**, 485301 (2010).
[41] K. Pi, K. M. McCreary, W. Bao, W. Han, Y. F. Chiang, Y. Li, S.W. Tsai, C. N. Lau, R. K. Kawakami, Phys. Rev. B **80**, 075406 (2009).
[42] S. Marchini, S. Günther, J. Wintterlin, Phys. Rev. B **76**, 075429 (2007).
[43] A. T. N'Diaye, S. Bleikamp, P. J. Feibelman, T. Michely, Phys. Rev. Lett. **97**, 215501 (2006).
[44] A. Varykhalov, J. Sánchez-Barriga, A. M. Shikin, C. Biswas, E. Vescovo, A. Rybkin, D. Marchenko, O. Rader, Phys. Rev. Lett. **101**, 157601 (2008).
[45] A. Grüneis, D. V. Vyalikh, Phys. Rev. B **77**, 193401 (2008).